Earth and Planetary Science Letters 494 (2018) 60–68

Contents lists available at ScienceDirect

Earth and Planetary Science Letters

www.elsevier.com/locate/epsl

A kinematic model for the evolution of the Eastern California Shear Zone and Garlock Fault, Mojave Desert, California

Timothy H. Dixon *, Surui Xie

School of Geosciences, University of South Florida, Tampa, FL, USA

ARTICLE INFO

Article history:
Received 27 December 2017
Received in revised form 21 April 2018
Accepted 25 April 2018
Available online xxxx
Editor: R. Bendick

Keywords:
Eastern California Shear Zone
kinematic model
Garlock fault
slip rate
total displacement

ABSTRACT

The Eastern California shear zone in the Mojave Desert, California, accommodates nearly a quarter of Pacific–North America plate motion. In south-central Mojave, the shear zone consists of six active faults, with the central Calico fault having the fastest slip rate. However, faults to the east of the Calico fault have larger total offsets. We explain this pattern of slip rate and total offset with a model involving a crustal block (the Mojave Block) that migrates eastward relative to a shear zone at depth whose position and orientation is fixed by the Coachella segment of the San Andreas fault (SAF), southwest of the transpressive "big bend" in the SAF. Both the shear zone and the Garlock fault are assumed to be a direct result of this restraining bend, and consequent strain redistribution. The model explains several aspects of local and regional tectonics, may apply to other transpressive continental plate boundary zones, and may improve seismic hazard estimates in these zones.

1. Introduction

Relative motion between the Pacific and North America plates in the southwestern US is accommodated either by the San Andreas fault in California, or the Eastern California shear zone (ECSZ), sometimes termed the Walker Lane north of the Garlock fault (Sauber et al., 1986, 1994; Dokka and Travis, 1990a,b; Dixon et al., 1995, 2000, 2003; Wesnousky, 2005; Lifton et al., 2013; Thatcher et al., 2016) (Fig. 1). The shear zone formed or accelerated when the southern part of the plate boundary jumped inland to form the modern Gulf of California, resulting in the transpressional "big bend" in the San Andreas fault (Atwater and Stock, 1998; Oskin and Stock, 2003; McQuarrie and Wernicke, 2005). This restraining bend causes high compressional and shear stresses in the adjacent crust, and influences many aspects of regional tectonics. In particular, the shear zone acts as a stress and strain bypass to the restraining bend (e.g., Liu et al., 2010; Plattner et al., 2010). The shear zone is also closely linked to a change in motion of the Sierra Nevada block (north of the Mojave block) in Late Miocene time, from a mainly westward direction relative to stable North America, associated with Basin and Range extension, to its current northwesterly direction (Atwater and Stock, 1998; Wernicke and Snow, 1998). Marine incursion into the northern Gulf of California is dated at 6.2 ± 0.2 Ma (Bennett et al., 2015) and it is likely that the shear zone formed or accelerated around or shortly before this time, i.e., 6–8 Ma (Oskin and Stock, 2003). McQuarrie and Wernicke (2005) place shear zone initiation somewhat earlier, 10–11 Ma. This relative youth, combined with excellent exposures in the arid southwestern US, make the shear zone an important "natural laboratory" for the study of fault evolution and earthquake hazard, especially for complex continental plate boundary zones and restraining bends.

There is an interesting contrast between the expression of the shear zone north and south of the Garlock fault (Fig. 1). North of the Garlock fault, the shear zone consists of three well-defined transtensional fault zones that lie within extensional basins, the westernmost basins of the Basin and Range province. From east to west, these fault zones are the Death Valley–Furnace Creek – Fish Lake Valley fault zone, the Panamint Valley – Hunter Mountain–Saline Valley fault zone, and the Owens Valley–Airport Lake fault zone. South of the Garlock fault, there is little or no extension, no well-developed basins, and more numerous (six) but less mature (lower offset) active strike-slip faults. The Garlock fault reflects the differential extension between the two regions (Davis and Burchfiel, 1973), moving in a left-lateral sense at rate of ~5–7 mm/yr in its western and central sections, decreasing to the east (e.g., McGill et al., 2009; Ganev et al., 2012; Dolan et al., 2016). Curiously, the ECSZ does not exhibit obvious offset across the Garlock fault, although the Garlock fault is known to be active based on mapped Holocene offsets.

Another curious feature of the ECSZ in the Mojave Desert is a mismatch between the slip rates of the various faults compris-

* Corresponding author.
E-mail address: thd@usf.edu (T.H. Dixon).

https://doi.org/10.1016/j.epsl.2018.04.050
0012-821X/

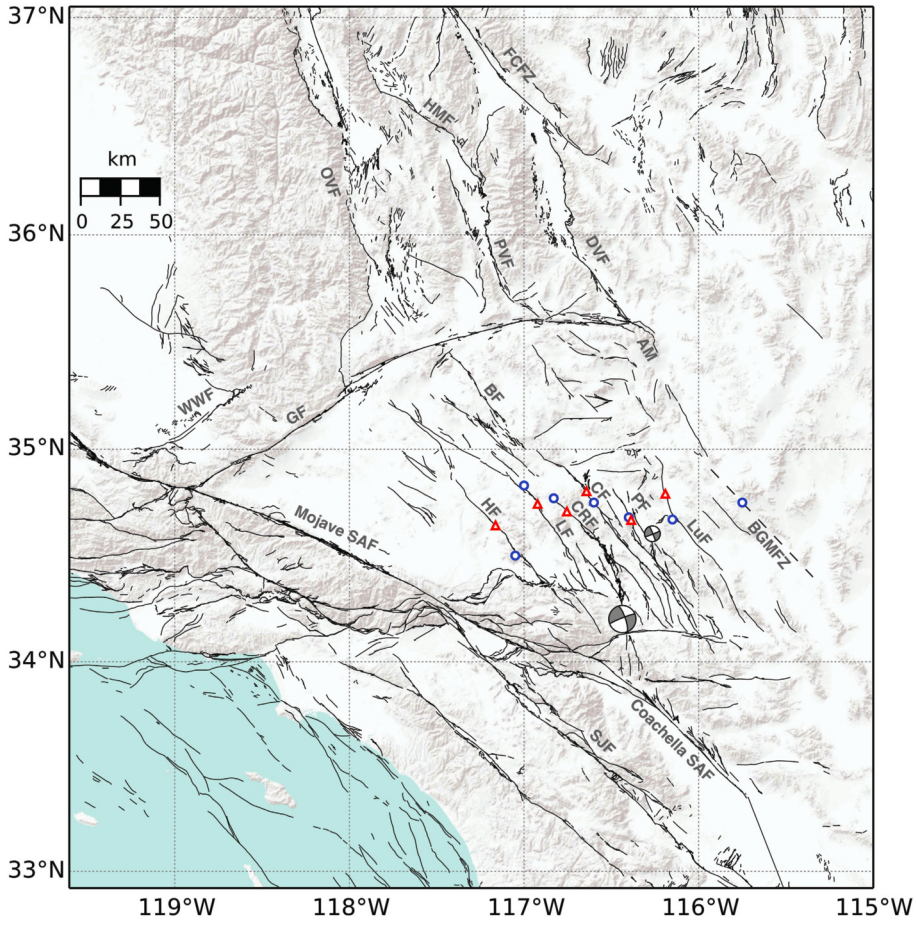

Fig. 1. Fault map of the study area. Red triangles represent locations of late Quaternary fault slip rate estimates (Oskin et al., 2008). Blue circles mark locations of total offset estimates (Miller and Morton, 1980; Dokka, 1983; Glazner et al., 2000; Jachens et al., 2002; Oskin et al., 2007; Lease et al., 2009; Andrew and Walker, 2017). Dashed line represents inferred fault trace of the Bristol–Granite Mountains Fault Zone (Lease et al., 2009). Beach balls mark the 1992 *Mw* 7.3 Landers and 1999 *Mw* 7.1 Hector Mine earthquakes (USGS Earthquake Hazards Program). Fault database from USGS and California Geological Survey. AM is Avawatz Mountains. Fault names are: BGMFZ – Bristol–Granite Mountains fault zone; Blackwater fault; CF – Calico fault; CRF – Camp Rock fault; Coachella SAF – Coachella section of the San Andreas fault; DVF – Death Valley fault; FCFZ – Furnace Creek fault zone; GF – Garlock fault; HF – Helendale fault; HMF – Hunter Mountain fault; LF – Lenwood fault; LuF – Ludlow fault; Mojave SAF – Mojave section of the San Andreas fault; WWF – White Wolf fault; OVF – Owens Valley fault; PVF – Panamint Valley fault; PF – Pisgah fault; SJF – San Jacinto fault. (For interpretation of the colors in the figure(s), the reader is referred to the web version of this article.)

ing the shear zone (highest on the central fault, the Calico fault, see Fig. 2a and Oskin et al. (2007, 2008)), and the total displacement on these faults (highest on the easternmost fault, the Bristol–Granite Mountains fault zone; Fig. 2b, Table S1). Dokka and Travis (1990a) suggested that there had a westward shift in the activity of ECSZ faults since their inception. In this paper, we present a simple kinematic model that explains these observations, as well as several other aspects of the regional tectonics.

2. Slip rate and total displacement data

2.1. Slip rate

Oskin et al. (2007, 2008) measured surface displacements and ages on six major dextral faults comprising the ECSZ (Helendale, Lenwood, Camp Rock, Calico, Pisgah, and Ludlow). These data suggest that the central (Calico) fault has the fastest slip rate (Fig. 2a), and the overall summed slip rate for the six faults is $\leq 6.2 \pm 1.9$ mm/yr significantly slower than the cumulative deformation rate across the shear zone derived from geodetic data (e.g., Sauber et al., 1994; Liu et al., 2015). Some authors have explained this difference by off-fault deformation: part of the total slip that occurs during earthquakes is not manifested by on-fault displacement, thus slip rates estimated by geologic methods using offset markers along surface fault traces could miss significant displacement (Shelef and Oskin, 2010; Herbert et al., 2014). Dolan and Haravitch (2014) suggest that off-fault deformation is likely to be more significant for low offset "immature" faults compared to large offset mature faults. Given that all six active faults studied by Oskin et al. (2007, 2008) have total offset <15 km (Fig. 2b), these are immature faults using the criterion of Dolan and Haravitch (2014). Hence, off-fault deformation is likely to be significant.

By studying deformed geologic features at several sites in the Mojave ECSZ, Shelef and Oskin (2010) found that off-fault deformation over zones of 1–2 km width accommodates 0 to ~25% of the total displacement, decreasing away from the fault. In a broader study, Herbert et al. (2014) used a boundary element model to suggest that off-fault deformation accounts for $40\% \pm 23\%$ of the total strain across the ECSZ. If we assume that this latter ratio is representative, and scale the slip rates for all active ECSZ fault (Table S1) then the cumulative deformation rate across the ECSZ is 10.3 ± 5.1 mm/yr (60%, or 6.2 mm/yr, is accommodated by well-defined active faults, and 40%, or 4.1 mm/yr, is accommodated as off-fault deformation and unmapped minor faults). This rate is equivalent within uncertainties to the rate estimated from geodetic data, both for the Mojave section and for the shear zone north of the Garlock fault (Dixon et al., 2000; Miller et al., 2001; Lifton et al., 2013; Xie et al., 2018). Wetmore et al. (2017) and

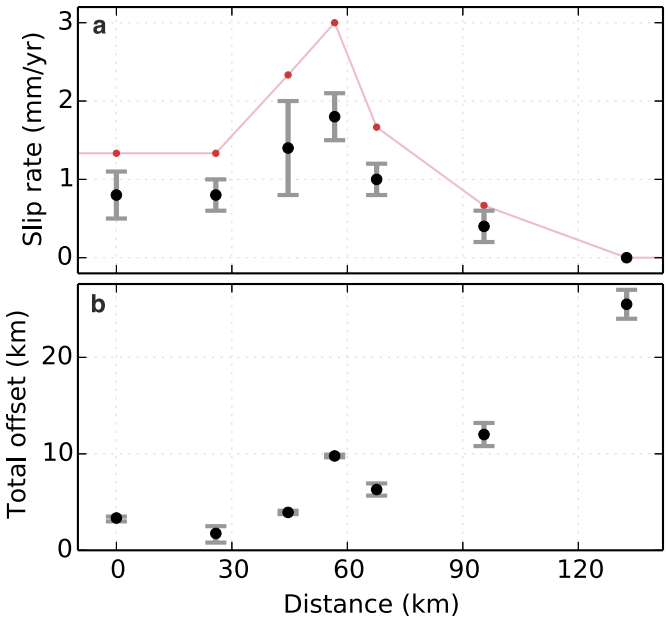

Fig. 2. Present-day slip rates and total offsets for several major faults comprising the ECSZ in the southern and central Mojave Desert. Distance is calculated across Pacific–North America plate motion direction from west to east, starting at the Helendale fault (Supplementary Fig. S1). Data for slip rates in (a) (Supplementary Table S1) are from Oskin et al. (2008) (black dots with error bar) and inferred value for BGMFZ (0 mm/yr, black dot without error bar) based on evidence for inactivity (Bedford et al., 2006). Red dots are scaled slip rates assuming 40% off-fault deformation (Herbert et al., 2014). Where multiple values are reported, the unweighted mean is used as the best estimate, and the range indicates uncertainty. For single values, if no uncertainty is reported, uncertainty is assumed to be ±10%. Additional details are given in Table S2.

Xie et al. (2018) report preliminary surface exposure ages of a large (1110 m) offset Pleistocene alluvial fan on the Calico fault, suggesting a slip rate averaged over the last few hundred thousand years of 3.2 ± 0.4 mm/yr, consistent with Oskin et al. (2008)'s result that the Calico fault has the fastest slip rate among ECSZ faults. While more work is required to validate the apparent agreement between geodetic results and the "adjusted" geological slip rates (after accounting for off-fault deformation and a possibly faster Calico fault) this agreement encourages us to consider simple uniformitarian models, with a constant ECSZ slip rate (summed across all faults) for the last few million years.

In the model to be presented, we use published geological slip rates (Fig. 2a) to scale the relative slip rates among the various ECSZ faults; in the event that off-fault deformation is in the range of 40%, then our model recovers the full or close to full rate for all time periods considered. If off-fault deformation is less, the model makes predictions of slip rate history and fault initiation time that are still useful, but predicts slip rates that would faster than the current rate, and predicts initiation times that would be later than the actual initiations times.

2.2. Total displacement

Fig. 2b and Table S2 summarize the fault displacement data used in this study. Pertinent points are summarized here. By using surface markers from an early Miocene structural belt, Dokka (1983) estimated total displacements on some of the major active faults across the central Mojave Desert, obtaining offsets between 1.5 and 14.4 km. Based on offset crustal magnetic anomaly pairs, Jachens et al. (2002) estimated 12.0 km displacement for the Ludlow fault. At the eastern margin of the ECSZ, Lease et al. (2009) found a minimum 24 km dextral offset based on reconstruction of a paleo-valley along the Bristol–Granite Mountains fault zone. Geologic data suggest that this fault is currently inactive (Bedford et al., 2006). Thus, the Bristol–Granite Mountains fault zone was likely an active part the ECSZ in the past, but has since become inactive (Lease et al., 2009). From Table S2, the cumulative displacement for all ECSZ faults sums to ∼63 km, close to the cumulative offset estimates of Dokka and Travis (1990a) (65 km), Glazner et al. (2002) (45–60 km) and Lease et al. (2009) (67 km).

3. Model description

We propose an evolutionary model for the Mojave section of the ECSZ that reconciles the observation that the fault with the fastest present-day slip rate (Calico fault) is not the fault with the largest total displacement. Our model builds on earlier suggestions that the ECSZ is part of a major through-going sub-crustal fault system extending from the southern part of the San Andreas fault (SAF) to northern Owens Valley, accommodating a significant fraction of Pacific–North America plate motion in this region (Dokka and Travis, 1990a,b; Savage et al., 1990). The model involves east-southeast displacement of the Mojave block relative to the adjacent Pacific plate, but a relatively fixed zone of shear at depth that is closely linked to the Coachella segment of the SAF to the south, presumably in the ductile lower crust/upper mantle. New faults form at pre-existing weaknesses in the brittle upper crust of the Mojave block as it passes through and over this zone of active shear (Fig. 3). Once a fault has moved out of this active zone, its slip rate goes to zero and its offset is fixed (Fig. 4). The model relies on three main assumptions:

1) The ECSZ is kinematically and dynamically linked to Pacific–North America plate motion and the big bend in the SAF, as suggested by many previous authors (e.g., Dokka and Travis, 1990a,b; Savage et al., 1990; Thatcher et al., 2016; Ye and Liu, 2017) and its average strike is closely aligned with the direction of Pacific–North America motion (Supplementary Fig. S1). The southern limit of the ECSZ is thus defined by the point where the SAF changes strike from northwest-southeast to west-northwest–east-southeast, i.e., near the restraining bend at the northern end of the Coachella section of the SAF, whose strike is about the same as the direction of Pacific–North America plate motion (DeMets and Merkouriev, 2016) (Supplementary Fig. S1). Relative to regions southwest of the Mojave section of the SAF, the Mojave block moves south-southeast with a speed equivalent to the SAF slip rate here (34 mm/yr, estimated from UCERF3, Field et al., 2013). Assuming the big bend is oriented approximately 30° from the plate motion direction, the component of block motion perpendicular to plate motion is about 17 mm/yr. We use this as the block migration rate relative to the shear zone at depth, assumed to be "pinned" to the Coachella segment of the SAF.
An important corollary is the assumption of steady state conditions: since Pacific–North America motion has been essentially constant over the last few million years (e.g., Atwater and Stock, 1998; DeMets and Dixon, 1999; DeMets and Merkouriev, 2016), we similarly assume that ECSZ motion has been steady on time scales of 10^4 years or long over the same period. Shorter term variation on individual faults (e.g., Dolan et al., 2007), is not precluded by our model. DeMets and Merkouriev (2016) suggest that the Pacific–North American plate rate has varied by less than 2% since 8 Ma, while plate direction has changed by several degrees; both are insignificant for purposes of our study. While the surficial expression of the shear zone continues to evolve (e.g., Dixon et al., 1995) and individual faults may accommodate varying amounts of shear at different times, we assume that the underlying shear zone, both north and south of the Garlock fault, has accom-

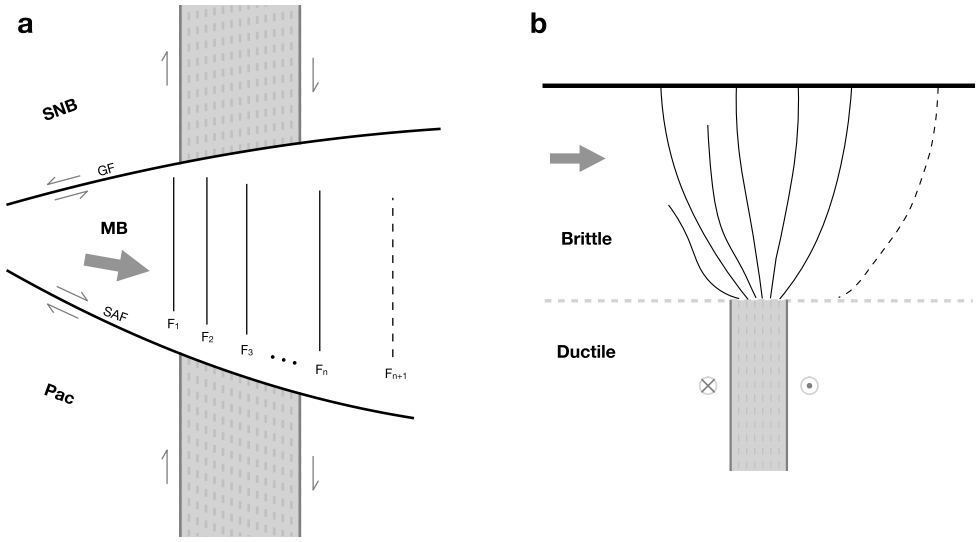

Fig. 3. (**a**) Map view cartoon illustrating ECSZ model. Grey shaded areas represent shear zones south and north of the Mojave block. F_1–F_n are faults within the active portion of the ECSZ, F_{n+1} represents a fault that has moved out of the shear zone and is currently inactive. Pac – Pacific plate; SNB – Sierra Nevada block; MB – Mojave block. (**b**) Cross-section view of ECSZ model. Grey shaded area shows the dextral shear zone at depth. Faults form when passing above the shear zone. Dashed line represents a fault that has moved out of the shear zone and is inactive.

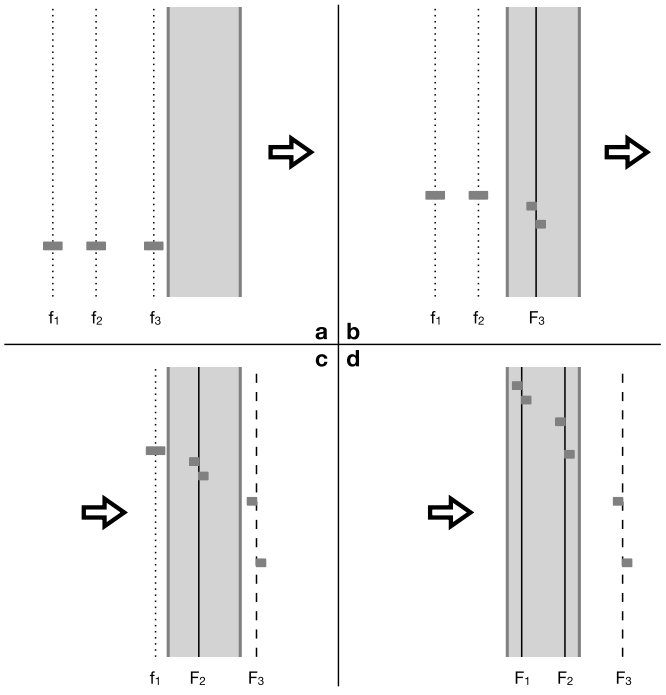

Fig. 4. Map-view cartoon showing time evolution of the shear zone and offset accumulation across individual faults for our ECSZ model. Grey shaded area shows active shear domain, relatively fixed above the shear zone at depth. Dark grey bars represent dikes or other features in the migrating upper crust that can become offset markers when displaced by faulting. Dotted lines represent weak zones that have not yet become faults yet (lower case f_1–f_3). Solid lines represent active faults (upper case F_1–F_3). Dashed line indicates a fault that has become inactive (F_3 in c and d).

modated an average of 10–12 mm/yr of northwest-directed dextral shear for the last few million years.

2) North of the Garlock fault, the Walker Lane straddles a rheologic boundary, clearly seen in heat flow data (Dixon et al., 2000), and presumably associated with Basin and Range extension and thinned lithosphere (Lachenbruch et al., 1994; Fliedner and Ruppert, 1996). Exploitation of this weakened lithosphere by the shear zone has localized shear within the ductile lower crust and uppermost mantle (e.g., Plattner et al., 2010; Liu et al., 2010), and promotes a few well-developed faults in the overlying brittle upper crust (Fig. 3b). Strain weakening stabilizes the position of the shear zone in both the upper and lower crust on time scales of a few million years unless the kinematic boundary conditions change significantly. Since the Mojave block has not experienced the same amount of extension, it lacks well-defined lithospheric-scale weak zones, perhaps contributing to its more complex fault mosaic. Nevertheless, the relatively fixed location of the shear zone to the north (eastern boundary of the Sierra Nevada block) and south (Coachella section of the SAF) constrains the locus of shear within the Mojave block at any given time.
3) Left-lateral motion across the Garlock fault means that the Mojave block translates eastward relative to the Sierra Nevada block. Right lateral motion across the SAF on the Mojave block's southern boundary means that the Mojave block also has an eastward component of motion relative to the Pacific plate. Regardless of reference frame, upper crustal faults in the Mojave Block that accommodate right-lateral shear eventually become misaligned with respect to the shear zones to the north and south (Fig. 3a). Once this occurs, the easternmost shear zone faults in the Mojave block are abandoned, and new faults form to the west in order to accommodate on-going shear. We further assume that the Garlock fault was active by the time the big bend formed, and may have formed at about the same time (Burbank and Whistler, 1987; Monastero et al., 1997). Hence the Garlock fault has likely influenced ECSZ evolution for all or most of the period of ECSZ activity.

Fig. 3b shows a cross-section view of the model, with a narrow zone of right-lateral shear at depth. When the brittle upper crust passes over this ductile shear zone, new faults form when stress is sufficient to cause displacement on pre-existing weaknesses, some of which coalesce and reach the surface. Once a fault has migrated out of this zone of shear, it becomes inactive and accumulates no more displacement (dashed line in Fig. 3).

Our model permits a quantitative derivation of slip rate and total offset history for the seven faults in the Mojave ECSZ, with a few additional assumptions. For simplicity slip is assumed to be localized onto individual faults (i.e., off-fault deformation is zero,

and all slip is fault-accommodated) and slip rate on each fault is scaled such that the cumulative slip rate is 10.3 mm/yr and remains constant:

$$V_{ECSZ} = \sum_{k=0}^{n} R_{k,t} \quad (1)$$

where V_{ECSZ} is the cumulative slip rate (10.3 mm/yr), $R_{k,t}$ is the slip rate of the k-th fault at time t before present, and n is the number of active faults at time t. Due to changes in the number of faults and their locations relative to the shear zone at depth, the slip rate of an individual fault is treated as a variable to satisfy the overall constant cumulative slip rate and slip distribution shown in Fig. 2:

$$R_{k,t} = s_t(a_l l_{k,t} + b_l) \quad (2)$$

where $l_{k,t}$ is the location of the k-th fault at time t, represented by the across-shear zone distance (x-axis in Fig. 2), and a_l and b_l are coefficients of a piecewise function (shown by the pink line in Fig. 2a) at the corresponding location, derived from the geologic slip rate. To the west of the current Helendale fault location, the piecewise function is derived by extending the function between the Helendale and Lenwood faults. A scaling factor s_t is used to ensure that the total slip rate is constant, in the sense that the historical slip rate function will have the same shape as present, but with different amplitude (Fig. S2). Due to limited data, we implement a piecewise function to reconstruct slip history. A smoother slip rate distribution function (e.g., a bell-shaped distribution) would give a smoother solution. Our model essentially assumes that for a given period with a fixed number of active faults, fault slip rates increase when moving towards the centerline of the shear zone, and decrease when moving away from the shear zone. Historical location $l_{k,t}$ of the k-th fault in equation (2) is calculated using:

$$l_{k,t} = l_{k,0} - V_{MB}t \quad (3)$$

where $l_{k,0}$ is the current location of the k-th fault, and V_{MB} is the across-shear zone speed of the Mojave Block (~17 mm/yr). At a given time t before present, total displacement ($D_{k,t}$) for the k-th fault is given by:

$$D_{k,t} = D_{k,0} - \int_0^t R_{k,t}dt \quad (4)$$

where $D_{k,0}$ is the current displacement of the k-th fault.

We reconstruct historic fault location, slip rate and total displacement from the present time back to the initiation time for each fault using equations (1)–(4), assuming positivity (no-left-lateral motion is allowed) and a constant cumulative slip rate. Time step size in the integration of equation (4) is ≤1 ka (typically 1 ka, <1 ka at times when new faults initiated). A different step size would not change the solutions significantly. Fig. 5 shows the reconstructed slip histories. Step changes are due to changes in the number of active faults. Fig. S3 shows slip rate versus historical location of these faults. While the solutions are model-dependent, they do satisfy all available data on fault location, total displacement, current summed slip rate across the ECSZ, and the current slip rate of individual faults, adjusted for an assumed value of off-fault deformation as described above.

The model reconstructions allow some aspects of fault evolution, such as initiation time and maximum slip rate, to be quantified. For example the Lenwood fault initiated most recently, ca. ~1.3 Ma. Based on the piecewise slip rate distribution

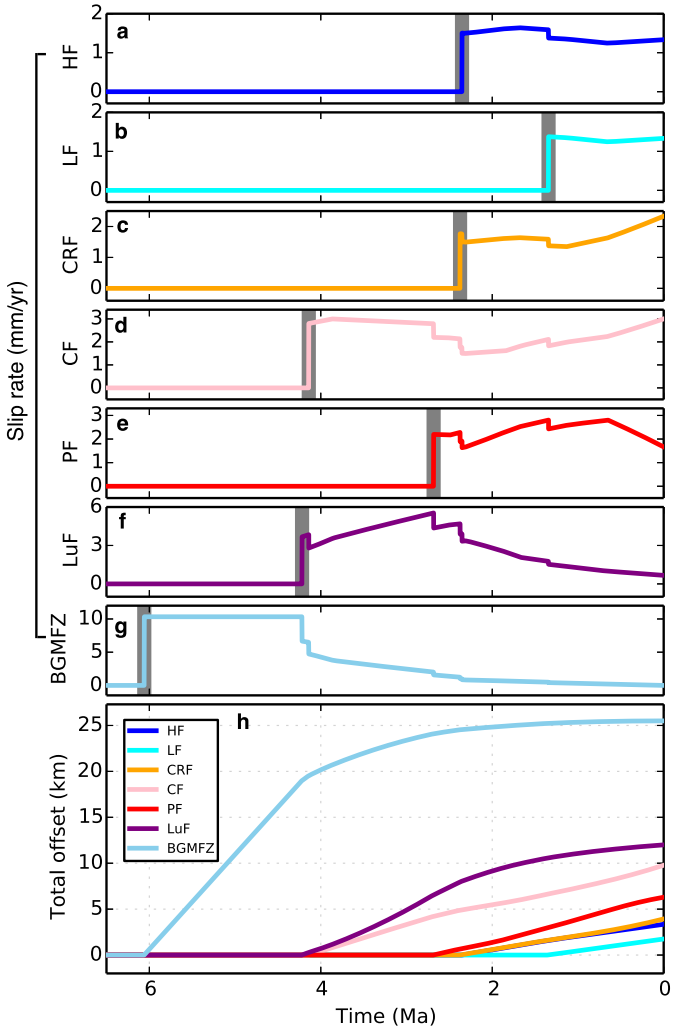

Fig. 5. Slip rate and total offset as a function of time for the seven faults in the Mojave Desert ECSZ. Top, a–g: Fault slip rate history based on total offsets and present-day slip rates. Grey line marks the initiation time for each fault. Base, h: Displacement history for individual faults, displacement at zero age is mapped total offset.

function used in our model, slip rate of the currently inactive Bristol–Granite Mountains fault zone decreased gradually after it passed the current location of the Ludlow fault. However, it could have become inactive at any location prior to arriving at its present location; the slip rates of other active faults would increase accordingly. Nevertheless, the Bristol–Granite Mountains fault zone was once the dominant fault in the ECSZ, accommodating >10 mm/yr slip for some period of time prior to becoming inactive.

4. Discussion

The likelihood of a major earthquake on a given fault is related to the slip rate of that fault. Discrepancies between slip rate estimates for a given fault, as determined by different techniques or over different time intervals, are therefore important, and signal one of two things: Either our knowledge of slip rate is imperfect, i.e., the discrepancy is not real, but rather an artifact of incomplete or poor data; or seismic hazard is increasing or decreasing with time, depending on whether the slip rate is increasing or decreasing with time, so that only the present-day slip rate is relevant. Many studies have therefore focused on the origin of slip rate dis-

crepancies (e.g., Minster and Jordan, 1987; Bennett et al., 2004; Brown et al., 2005; Oskin et al., 2008; Thatcher, 2009; Cowgill et al., 2009; Mohadjer et al., 2017).

Our kinematic model provides a simple explanation for a number of observations in the Mojave Desert region of California, including the time-variable slip rates that characterize several ECSZ faults (e.g., Oskin and Iriondo, 2004). It also explains other key features of local and regional tectonics, including:

1) Why the Calico fault has the fastest slip rate (it currently lies in the center of the shear zone, where shear strain rates are highest);
2) Why the presently fastest fault (Calico fault) does not have the largest total offset (it is younger than some faults to the east, and hence has had less time to accumulate displacement);
3) Why total offset increases to the east (eastern faults initiated earlier and experienced longer periods of slip);
4) Why the fault with the largest offset (Bristol–Granite Mountains fault zone) is not currently active (it has moved out of the active zone of shear);
5) Why faults east of the Calico fault have present-day slip rates that are less than longer-term average slip rates (they have move away for the central high strain rate part of the shear zone);
6) Why the shear zone in the Mojave Desert is not displaced in a left-lateral sense as it crosses the Garlock fault (it continually reforms by activating new upper crustal faults);
7) Why ECSZ faults do not cross the Garlock fault (southeast translation of the Mojave block moves ECSZ faults away from the Garlock fault, hence the faults must continually propagate to the northwest).
8) Why ECSZ faults in the Mojave Desert are less mature than their counterparts north of the Garlock fault (individual faults have been active for less time, and therefore have accumulated less total offset).

Net eastward motion of the Mojave Block relative to the Sierra Nevada block (of order 30 km assuming it has been going on for 5 million years) may promote formation of several pull-apart basins near the block's western boundary. A particularly well-developed one is located immediately east of the intersection of the Garlock and San Andreas faults (Jachens et al., 2002). This basin is not clear in topographic data because it is filled with sediments derived from high-relief areas to the west (Supplementary Fig. S4). However regional gravity data show a strong negative isostatic gravity anomaly here, consistent with a basin filled with lower density sediments (Supplementary Fig. S5). This area is also characterized by several recent normal fault earthquakes, with focal mechanisms consistent with east-southeast–west-northwest directed extension (Supplementary Fig. S6). A simple model involving extension on a listric normal fault (Supplementary Fig. S5) suggests about 20 ± 5 km of west-east or west-northwest–east-southeast extension on the modeled basin. Corresponding compressional deformation on the block's eastern boundary is much less – the Garlock fault ends in the Avawatz mountains south of Death Valley in a series of small thrust faults with north-south strikes (Fig. 1 and Duvall et al., 2017). The contrast in deformation style on the block's western and eastern boundaries reflects the block's motion relative to stable North America. In other words, the Pacific plate, the Sierra Nevada block, and the Mojave block all experience a component of westward motion relative to stable North America, but the Mojave block has the lowest westward velocity component in this reference frame. Thus, it experiences significant extensional deformation on its western boundary, but only modest contractional deformation on its eastern boundary.

Our model ignores several aspects of shear zone evolution and regional tectonics, for example, the rotational aspects of regional deformation, which could influence fault re-orientation (e.g., Luyendyk, 1991; Nur et al., 1993), although Valentine et al. (1993) note that post-10 Ma rotation in most of the Mojave block is small. We also assume that the shear zone is a relatively stationary feature north of the Garlock fault. However, this section of the shear zone also experiences displacement relative to the Coachella section of the San Andreas fault, albeit at lower rates compared to the Mojave block, potentially influencing its evolution in similar ways. For example, the easternmost of the three major dextral fault zones north of the Garlock fault, the Death Valley–Furnace Creek fault zone, has large total offset (68 ± 4 km; Snow and Wernicke, 1989) and was likely active by at least 6–8 Ma. In contrast, the Hunter Mountain–Panamint Valley system to the west has a much smaller offset (9.3 ± 1.4 km; Burchfiel et al., 1987) and a much younger initiation age, ~2.8 Ma (Lee et al., 2009). Finally, we assume that the rate of dextral shear across the shear zone has been constant over the last few million years. Evolution of the Elsinore and San Jacinto faults during this period could have "bled off" some of the compressional stresses associated with the big bend, perhaps reducing the rate of dextral shear on the shear zone.

Our model does not specify the depth extent of the shear zone or the thickness of the translating Mojave crust. Rather than the entire crust or lithosphere, it is possible that only the brittle upper crust of the Mojave block translates east relative to the shear zone, separated from the ductile lower crust by a mid-crustal decollement. Fuis et al. (2007) describe evidence for such a feature based on active and passive seismic imaging. The mid-crustal decollement allows the upper crust to escape laterally with minimal deformation, despite strong contractional stresses. The lower crust would thicken or be subducted in this model, forming a crustal root.

Our kinematic model also does not specify the stresses that drive the Mojave Block's relative eastward motion, which could be driven from below or from the side. Bartley et al. (1990) and Jackson (1992) first pointed out that north-south contraction in a deforming continental zone could lead to lateral extrusion of a crustal block (side-driven model), accommodated by paired left-lateral and right-lateral faults (Fig. 3a in Jackson, 1992); such a model could apply to the Mojave, with north-south contraction associated with the big bend driving the block's relative eastward motion via tectonic escape (e.g., Dolan et al., 2007). Formation of the Garlock fault would thus be closely connected with formation of the big bend, a model that is consistent with limited age data (Burbank and Whistler, 1987; Monastero et al., 1997). Compressional stresses associated with the transpressional big bend are therefore accommodated in two main ways in this model: thrust faulting south of the bend, on faults that strike mostly parallel to the big bend, e.g., in the Los Angeles basin, and strike slip faulting north of the bend on the Garlock fault, nearly perpendicular to the bend, accommodating lateral escape of the Mojave Block.

The Garlock fault plays a dual role in the kinematics of the Mojave Block. In addition to accommodating lateral escape, it also accommodates differential extension between the Mojave Block and the Sierra Nevada block. The latter experiences a component of west-directed extension relative to stable North America, reflecting summed extension across three major valleys: Owens Valley, Panamint Valley, and Death Valley (Fig. 1). The Garlock fault slip rate therefore decreases eastward, reaching zero by the time it is east of Death Valley (Fig. 1). The Mojave Block lacks such well-defined extensional valleys, perhaps reflecting the relative eastward "push" it experiences associated with its lateral escape.

Our explanation for the long-term southeastward motion of the Mojave Block relative to the Pacific plate and initial formation of the Garlock fault also has implications for the long-term evolution

of that fault. Since the Garlock fault by definition is the northwest boundary of the Mojave block, forming at the location where the San Andreas fault changes strike to form the big bend, the boundary fault must continually reform to the northwest as the block migrates to the southeast. The White Wolf fault, ~30 km northwest of the Garlock fault (Fig. 1) may represent the future northern boundary of the Mojave Block.

While the current slip rate of an active fault is a key variable in seismic hazard estimation, there are several challenges to its accurate estimation in rapidly evolving plate boundary zones:

1) Is a given fault currently active?
2) If so, what is its present slip rate?
3) Is the fault accelerating, such that past activity may not predict future earthquake potential?
4) Could rapid evolution of the broader plate boundary zone lead to spatial complexity, and earthquakes on previously unmapped faults with limited surface expression?

Many continental plate boundary zones experiencing transpressional tectonics exhibit complexity on par with SAF big bend–ECSZ system. Aspects of our model may apply to these systems. Fuis et al. (2007) have called attention to similarities between the SAF big bend–ECSZ system and South Island, New Zealand. Another example is the Arabia–Eurasia collision zone, where the Arabian plate moves north and collides with Eurasia. Westward extrusion of the Anatolian block in response to this collision via paired right-lateral (North Anatolian fault) and left-lateral (East Anatolian fault) is well known (e.g., Jackson, 1992). The region to the east experiences eastward block extrusion (Jackson, 1992, and Supplementary Fig. S7) and has been the site of numerous deadly earthquakes on previously unmapped or poorly mapped faults. These include the 26 December 2003 *Mw* 6.6 Bam earthquake, the deadliest earthquake of 2003, killing approximately 30,000 people (Talebian et al., 2004; Fialko et al., 2005) and the 12 November 2017 *Mw* 7.3 earthquake near the Iran–Iraq border, the deadliest earthquake of 2017, killing more than 600 people. Eastern Iran in particular bears strong similarity to our study area, with northward convergence of the Arabian plate helping to drive eastward extrusion of the Lut block (Berberian, 2005; Walker et al., 2013). The block is bounded to the north by the left-lateral east-west striking Doruneh fault, analogous to the Garlock fault, and is cut by numerous right lateral, north-south striking strike-slip faults in the central and eastern portions of the block, analogous to the ECSZ. Many of these faults have limited displacement and are poorly expressed at the surface, a characteristic of immature faults and a direct prediction of our model. One of these faults was responsible for the deadly Bam earthquake (Supplemental Fig. S7)

5. Conclusions

We have presented a simple kinematic model for the evolution of the eastern California shear zone (ECSZ) that builds on early suggestions that the shear zone is a through-going sub-crustal fault system extending from the southern San Andreas fault to northern Owens Valley, a distance of about 500 km. The model assumes that shear zone formation is closely linked to Pacific–North America plate motion and the inland jump of the plate boundary in mid-Miocene time to form the Gulf of California, and consequent formation of the transpressive "big bend" of the San Andreas fault (SAF), immediately north of the Coachella section of the SAF. Motivated by the observation that Pacific–North America motion has been relatively steady for the last few million years, we assume that ECSZ motion has been similarly steady during this time, accommodating 10–12 mm/yr of northwest-directed dextral shear. In contrast to the steadiness of underlying shear, the surficial expression of faults that manifest this shear is a complex mosaic, especially in the Mojave block, which moves east-southeast relative to the Coachella section of the SAF. This relative motion eventually causes some ECSZ faults to become mis-aligned with the underlying shear zone and be abandoned. A kinematic model involving a constant translation rate explains many features of the local and regional tectonics, including the present pattern of slip rates (highest in the central fault within the shear zone, the Calico fault) and total offsets (highest in the currently inactive Bristol–Granite Mountains fault zone to the east). Our model may apply to other transpressive continental plate boundary zones, including parts of the Arabia–Eurasia collision zone, and may improve seismic hazard estimates in these regions.

Acknowledgements

This research was supported by USGS-NEHRP grant G16AP00102 to THD. SX acknowledges a USF Tharp endowed scholarship. We thank Paul Wetmore, Rocco Malservisi, Lewis Owen and Charles Connor for discussions, and Mian Liu and an anonymous reviewer for detailed comments that greatly improved the manuscript. Fault database used in Fig. 1 was from U.S. Geological Survey and California Geological Survey (http://earthquakes.usgs.gov/hazards/qfaults/). The authors have no financial or other conflicts of interest with the views expressed in this paper.

Appendix A. Supplementary material

Supplementary material related to this article can be found online at https://doi.org/10.1016/j.epsl.2018.04.050.

References

Andrew, J.E., Walker, J.D., 2017. Path and amount of dextral fault slip in the Eastern California shear zone across the central Mojave Desert. Geol. Soc. Am. Bull. 129 (7–8), 855–868. https://doi.org/10.1130/B31527.1.

Atwater, T., Stock, J., 1998. Pacific–North America plate tectonics of the Neogene southwestern United States: an update. Int. Geol. Rev. 40 (5), 375–402. https://doi.org/10.1080/00206819809465216.

Bartley, J.M., Glazner, A.F., Schermer, E.R., 1990. North-south contraction of the Mojave block and strike-slip tectonics in southern California. Science 248 (4961), 1398–1401. https://doi.org/10.1126/science.248.4961.1398.

Bedford, D.R., Miller, D.M., Phelps, G.A., 2006. Preliminary surficial geologic map database of the Amboy 30 × 60 minute quadrangle, California. U.S. Geol. Surv. Open-File Report 2006–1165. https://pubs.usgs.gov/of/2006/1165/.

Bennett, R.A., Friedrich, A.M., Furlong, K.P., 2004. Codependent histories of the San Andreas and San Jacinto fault zones from inversion of fault displacement rates. Geology 32 (11), 961–964. https://doi.org/10.1130/G20806.1.

Bennett, S.E., Oskin, M.E., Dorsey, R.J., Iriondo, A., Kunk, M.J., 2015. Stratigraphy and structural development of the southwest Isla Tiburón marine basin: implications for latest Miocene tectonic opening and flooding of the northern Gulf of California. Geosphere 11 (4), 977–1007. https://doi.org/10.1130/GES01153.1.

Berberian, M., 2005. The 2003 Bam urban earthquake: a predictable seismotectonic pattern along the western margin of the rigid Lut block, southeast Iran. Earthq. Spectra 21 (S1), 35–99. https://doi.org/10.1193/1.2127909.

Brown, E.T., Molnar, P., Bourlès, D.L., 2005. Comment on "Slip-rate measurements on the Karakorum Fault may imply secular variations in fault motion". Science 309 (5739), 1326. https://doi.org/10.1126/science.1112508.

Burbank, D.W., Whistler, D.P., 1987. Temporally constrained tectonic rotations derived from magnetostratigiraphic data: implications for the initiation of the Garlock fault, California. Geology 15 (12), 1172–1175. https://doi.org/10.1130/0091-7613(1987)15<1172:TCTRDF>2.0.CO;2.

Burchfiel, B.C., Hodges, K.V., Royden, L.H., 1987. Geology of Panamint Valley–Saline Valley Pull-Apart System, California: palinspastic evidence for low-angle geometry of a Neogene Range-Bounding Fault. J. Geophys. Res., Solid Earth 92 (B10), 10422–10426. https://doi.org/10.1029/JB092iB10p10422.

Cowgill, E., Gold, R.D., Xuanhua, C., Xiao-Feng, W., Arrowsmith, J.R., Southon, J., 2009. Low Quaternary slip rate reconciles geodetic and geologic rates along the Altyn Tagh fault, northwestern Tibet. Geology 37 (7), 647–650. https://doi.org/10.1130/G25623A.1.

Davis, G.A., Burchfiel, B.C., 1973. Garlock fault: an intracontinental transform structure, southern California. Geol. Soc. Am. Bull. 84 (4), 1407–1422. https://doi.org/10.1130/0016-7606(1973)84<1407:GFAITS>2.0.CO;2.

DeMets, C., Dixon, T.H., 1999. New kinematic models for Pacific–North America motion from 3 Ma to present, I: evidence for steady motion and biases in the NUVEL-1A Model. Geophys. Res. Lett. 26 (13), 1921–1924. https://doi.org/10.1029/1999GL900405.

DeMets, C., Merkouriev, S., 2016. High-resolution reconstructions of Pacific–North America plate motion: 20 Ma to present. Geophys. J. Int. 207 (2), 741–773. https://doi.org/10.1093/gji/ggw305.

Dixon, T.H., Robaudo, S., Lee, J., Reheis, M.C., 1995. Constraints on present-day Basin and Range deformation from space geodesy. Tectonics 14 (4), 755–772. https://doi.org/10.1029/95TC00931.

Dixon, T.H., Miller, M., Farina, F., Wang, H., Johnson, D., 2000. Present-day motion of the Sierra Nevada block and some tectonic implications for the Basin and Range province, North American Cordillera. Tectonics 19 (1), 1–24. https://doi.org/10.1029/1998TC001088.

Dixon, T.H., Norabuena, E., Hotaling, L., 2003. Paleoseismology and Global Positioning System: earthquake-cycle effects and geodetic versus geologic fault slip rates in the Eastern California shear zone. Geology 31 (1), 55–58. https://doi.org/10.1130/0091-7613(2003)031<0055:PAGPSE>2.0.CO;2.

Dokka, R.K., 1983. Displacements on late Cenozoic strike-slip faults of the central Mojave Desert, California. Geology 11 (5), 305–308. https://doi.org/10.1130/0091-7613(1983)11<305:DOLCSF>2.0.CO;2.

Dokka, R.K., Travis, C.J., 1990a. Late Cenozoic strike-slip faulting in the Mojave Desert, California. Tectonics 9 (2), 311–340. https://doi.org/10.1029/TC009i002p00311.

Dokka, R.K., Travis, C.J., 1990b. Role of the eastern California shear zone in accommodating Pacific–North American plate motion. Geophys. Res. Lett. 17 (9), 1323–1326. https://doi.org/10.1029/GL017i009p01323.

Dolan, J.F., Bowman, D.D., Sammis, C.G., 2007. Long-range and long-term fault interactions in Southern California. Geology 35 (9), 855–858. https://doi.org/10.1130/G23789A.1.

Dolan, J.F., Haravitch, B.D., 2014. How well do surface slip measurements track slip at depth in large strike-slip earthquakes? The importance of fault structural maturity in controlling on-fault slip versus off-fault surface deformation. Earth Planet. Sci. Lett. 388, 38–47. https://doi.org/10.1016/j.epsl.2013.11.043.

Dolan, J.F., McAuliffe, L.J., Rhodes, E.J., McGill, S.F., Zinke, R., 2016. Extreme multi-millennial slip rate variations on the Garlock fault, California: strain supercycles, potentially time-variable fault strength, and implications for system-level earthquake occurrence. Earth Planet. Sci. Lett. 446, 123–136. https://doi.org/10.1016/j.epsl.2016.04.011.

Duvall, A.R., Cowan, D.S., Casale, G., Chinn, L., Fendick, A.M., Blythe, A.E., Reinert, E., 2017. Deformation history at the eastern end of the Garlock fault, CA from Avawatz mountains low temperature thermochronology. Abstract (Paper No. 55-8). In: GSA Annual Meeting. Seattle, WA. https://doi.org/10.1130/abs/2017AM-302486.

Fialko, Y., Sandwell, D., Simons, M., Rosen, P., 2005. Three-dimensional deformation caused by the Bam, Iran, earthquake and the origin of shallow slip deficit. Nature 435 (7040), 295–299. https://doi.org/10.1038/nature03425.

Field, E.H., Biasi, G.P., Bird, P., Dawson, T.E., Felzer, K.R., Jackson, D.D., Johnson, K.M., Jordan, T.H., Madden, C., Michael, A.J., Milner, K.R., Page, M.T., Parsons, T., Powers, P.M., Shaw, B.E., Thatcher, W.R., Weldon II, R.J., Zeng, Y., 2013. Uniform California earthquake rupture forecast, version 3 (UCERF3) – the time-independent model. U.S. Geol. Surv. Open-File Report 2013–1165. http://pubs.usgs.gov/of/2013/1165/.

Fliedner, M.M., Ruppert, S., Southern Sierra Nevada Continental Dynamics Working Group, 1996. Three-dimensional crustal structure of the southern Sierra Nevada from seismic fan profiles and gravity modeling. Geology 24 (4), 367–370. https://doi.org/10.1130/0091-7613(1996)024<0367:TDCSOT>2.3.CO;2.

Fuis, G.S., Kohler, M.D., Scherwath, M., Brink, U.T., Van Avendonk, H.J., Murphy, J.M., 2007. A comparison between the transpressional plate boundaries of South Island, New Zealand, and southern California, USA: the Alpine and San Andreas fault systems. In: Okaya, D., Stern, T., Davey, F. (Eds.), A Continental Plate Boundary: Tectonics at South Island. New Zealand American Geophysical Union, Washington, D.C.

Ganev, P.N., Dolan, J.F., McGill, S.F., Frankel, K.L., 2012. Constancy of geologic slip rate along the central Garlock fault: implications for strain accumulation and release in southern California. Geophys. J. Int. 190 (2), 745–760. https://doi.org/10.1111/j.1365-246X.2012.05494.x.

Glazner, A.F., Bartley, J.M., Sanner, W.K., 2000. Nature of the southwestern boundary of the central Mojave Tertiary province, Rodman Mountains, California. Geol. Soc. Am. Bull. 112 (1), 34–44. https://doi.org/10.1130/0016-7606(2000)112<34:NOTSBO>2.0.CO;2.

Glazner, A.F., Walker, J.D., Bartley, J.M., Fletcher, J.M., 2002. Cenozoic evolution of the Mojave block of southern California. Geologic evolution of the Mojave Desert and southwestern Basin and Range. Geol. Soc. Amer. Mem. 195, 19–41.

Herbert, J.W., Cooke, M.L., Oskin, M., Difo, O., 2014. How much can off-fault deformation contribute to the slip rate discrepancy within the eastern California shear zone? Geology 42 (1), 71–75. https://doi.org/10.1130/G34738.1.

Jachens, R.C., Langenheim, V.E., Matti, J.C., 2002. Relationship of the 1999 Hector Mine and 1992 Landers fault ruptures to offsets on Neogene faults and distribution of late Cenozoic basins in the Eastern California Shear Zone. Bull. Seismol. Soc. Am. 92 (4), 1592–1605. https://doi.org/10.1785/0120000915.

Jackson, J., 1992. Partitioning of strike-slip and convergent motion between Eurasia and Arabia in eastern Turkey and the Caucasus. J. Geophys. Res., Solid Earth 97 (B9), 12471–12479. https://doi.org/10.1029/92JB00944.

Lachenbruch, A.H., Sass, J.H., Morgan, P., 1994. Thermal regime of the southern Basin and Range Province: 2. Implications of heat flow for regional extension and metamorphic core complexes. J. Geophys. Res., Solid Earth 99 (B11), 22121–22133. https://doi.org/10.1029/94JB01890.

Lease, R.O., McQuarrie, N., Oskin, M., Leier, A., 2009. Quantifying dextral shear on the Bristol–Granite Mountains fault zone: successful geologic prediction from kinematic compatibility of the Eastern California Shear Zone. J. Geol. 117 (1), 37–53. https://doi.org/10.1086/593320.

Lee, J., Stockli, D.F., Owen, L.A., Finkel, R.C., Kislitsyn, R., 2009. Exhumation of the Inyo Mountains, California: implications for the timing of extension along the western boundary of the Basin and Range Province and distribution of dextral fault slip rates across the eastern California shear zone. Tectonics 28 (1). https://doi.org/10.1029/2008TC002295.

Lifton, Z.M., Newman, A.V., Frankel, K.L., Johnson, C.W., Dixon, T.H., 2013. Insights into distributed plate rates across the Walker Lane from GPS geodesy. Geophys. Res. Lett. 40 (17), 4620–4624. https://doi.org/10.1002/grl.50804.

Liu, M., Wang, H., Li, Q., 2010. Inception of the eastern California shear zone and evolution of the Pacific–North American plate boundary: from kinematics to geodynamics. J. Geophys. Res., Solid Earth 115 (B7). https://doi.org/10.1029/2009JB007055.

Liu, S., Shen, Z.K., Bürgmann, R., 2015. Recovery of secular deformation field of Mojave shear zone in southern California from historical terrestrial and GPS measurements. J. Geophys. Res., Solid Earth 120 (5), 3965–3990. https://doi.org/10.1002/2015JB011941.

Luyendyk, B.P., 1991. A model for Neogene crustal rotations, transtension, and transpression in southern California. Geol. Soc. Am. Bull. 103 (11), 1528–1536. https://doi.org/10.1130/0016-7606(1991)103<1528:AMFNCR>2.3.CO;2.

McGill, S.F., Wells, S.G., Fortner, S.K., Kuzma, H.A., McGill, J.D., 2009. Slip rate of the western Garlock fault, at Clark Wash, near Lone Tree Canyon, Mojave Desert, California. Geol. Soc. Am. Bull. 121 (3–4), 536–554. https://doi.org/10.1130/B26123.

McQuarrie, N., Wernicke, B.P., 2005. An animated tectonic reconstruction of southwestern North America since 36 Ma. Geosphere 1 (3), 147–172. https://doi.org/10.1130/GES00016.1.

Miller, F.K., Morton, D.M., 1980. Potassium–argon geochronology of the eastern Transverse Ranges and southern Mojave Desert, southern California. U.S. Geol. Surv. Prof. Pap. 1152. https://pubs.er.usgs.gov/publication/pp1152.

Miller, M., Johnson, D., Dixon, T.H., Dokka, R.K., 2001. Refined kinematics of the eastern California shear zone from GPS observations, 1993–1998. J. Geophys. Res. 106, 2245–2263. https://doi.org/10.1029/2000JB900328.

Minster, J.B., Jordan, T.H., 1987. Vector constraints on western U.S. deformation from space geodesy, neotectonics, and plate motions. J. Geophys. Res. 92, 4798–4804. https://doi.org/10.1029/JB092iB06p04798.

Mohadjer, S., Ehlers, T.A., Bendick, R., Mutz, S.G., 2017. Review of GPS and Quaternary fault slip rates in the Himalaya–Tibet orogen. Earth-Sci. Rev. 174, 39–52. https://doi.org/10.1016/j.earscirev.2017.09.005.

Monastero, F.C., Sabin, A.E., Walker, J.D., 1997. Evidence for post-early Miocene initiation of movement on the Garlock fault from offset of the Cudahy Camp Formation, east-central California. Geology 25 (3), 247–250. https://doi.org/10.1130/0091-7613(1997)025<0247:EFPEMI>2.3.CO;2.

Nur, A., Ron, H., Beroza, G.C., 1993. The nature of the Landers–Mojave earthquake line. Science 261 (5118), 201–203. https://doi.org/10.1126/science.261.5118.201.

Oskin, M., Stock, J., 2003. Pacific–North America plate motion and opening of the Upper Delfín basin, northern Gulf of California, Mexico. Geol. Soc. Am. Bull. 115 (10), 1173–1190. https://doi.org/10.1130/B25154.1.

Oskin, M., Iriondo, A., 2004. Large-magnitude transient strain accumulation on the Blackwater fault, Eastern California shear zone. Geology 32 (4), 313–316. https://doi.org/10.1130/G20223.1.

Oskin, M., Perg, L., Blumentritt, D., Mukhopadhyay, S., Iriondo, A., 2007. Slip rate of the Calico Fault: implications for geologic versus geodetic rate discrepancy in the eastern California shear zone. J. Geophys. Res., Solid Earth 112 (B3). https://doi.org/10.1029/2006JB004451.

Oskin, M., Perg, L., Shelef, E., Strane, M., Gurney, E., Singer, B., Zhang, X., 2008. Elevated shear zone loading rate during an earthquake cluster in eastern California. Geology 36 (6), 507–510. https://doi.org/10.1130/G24814A.1.

Plattner, C., Malservisi, R., Furlong, K.P., Govers, R., 2010. Development of the Eastern California Shear Zone–Walker Lane belt: the effects of microplate motion and pre-existing weakness in the Basin and Range. Tectonophysics 485 (1), 78–84. https://doi.org/10.1016/j.tecto.2009.11.021.

Sauber, J., Thatcher, W., Solomon, S.C., 1986. Geodetic measurement of deformation in the central Mojave Desert, California. J. Geophys. Res., Solid Earth 91 (B12), 12683–12693. https://doi.org/10.1029/JB091iB12p12683.

Sauber, J., Thatcher, W., Solomon, S.C., Lisowski, M., 1994. Geodetic slip rate for the eastern California shear zone and the recurrence time of Mojave Desert earthquakes. Nature 367 (6460), 264–266. https://doi.org/10.1038/367264a0.

Savage, J.C., Lisowski, M., Prescott, W.H., 1990. An apparent shear zone trending north-northwest across the Mojave Desert into Owens Valley, eastern

California. Geophys. Res. Lett. 17 (12), 2113–2116. https://doi.org/10.1029/GL017i012p02113.

Shelef, E., Oskin, M., 2010. Deformation processes adjacent to active faults: examples from eastern California. J. Geophys. Res., Solid Earth 115 (B5). https://doi.org/10.1029/2009JB006289.

Snow, J.K., Wernicke, B., 1989. Uniqueness of geological correlations: an example from the Death Valley extended terrain. Geol. Soc. Am. Bull. 101, 1351–1362. https://doi.org/10.1130/0016-7606(1989)101<1351:UOGCAE>2.3.CO;2.

Talebian, M., Fielding, E.J., Funning, G.J., Ghorashi, M., Jackson, J., Nazari, H., Parsons, B., Priestley, K., Rosen, P.A., Walker, R., Wright, T.J., 2004. The 2003 Bam (Iran) earthquake: rupture of a blind strike-slip fault. Geophys. Res. Lett. 31 (11). https://doi.org/10.1029/2004GL020058.

Thatcher, W., 2009. How the continents deform: the evidence from tectonic geodesy. Annu. Rev. Earth Planet. Sci. 37, 237–262. https://doi.org/10.1146/annurev.earth.031208.100035.

Thatcher, W., Savage, J.C., Simpson, R.W., 2016. The Eastern California Shear Zone as the northward extension of the southern San Andreas fault. J. Geophys. Res., Solid Earth 121 (4), 2904–2914. https://doi.org/10.1002/2015JB012678.

Valentine, M.J., Brown, L.L., Golombek, M.P., 1993. Cenozoic crustal rotations in the Mojave Desert from paleomagnetic studies around Barstow, California. Tectonics 12 (3), 666–677. https://doi.org/10.1029/92TC02813.

Walker, R.T., Bergman, E.A., Elliott, J.R., Fielding, E.J., Ghods, A.R., Ghoraishi, M., Jackson, J., Nazari, H., Nemati, M., Oveisi, B., Talebian, M., 2013. The 2010–2011 South Rigan (Baluchestan) earthquake sequence and its implications for distributed deformation and earthquake hazard in southeast Iran. Geophys. J. Int. 193 (1), 349–374. https://doi.org/10.1093/gji/ggs109.

Wernicke, B., Snow, J.K., 1998. Cenozoic tectonism in the central Basin and Range: motion of the Sierran-Great Valley block. Int. Geol. Rev. 40 (5), 403–410. https://doi.org/10.1080/00206819809465217.

Wesnousky, S.G., 2005. Active faulting in the Walker Lane. Tectonics 24 (3). https://doi.org/10.1029/2004TC001645.

Wetmore, P.H., Xie, S., Gallant, E., Owen, L.A., Dixon, T.H., 2017. A new geological slip rate estimate for the Calico fault, Eastern California: implications for geodetic versus geologic rate estimates in the Eastern California shear zone. Abstract (T51G-0553). In: 2017 AGU Fall Meeting. New Orleans, LA.

Xie, S., Gallant, E., Wetmore, P.H., Owen, L.A., Figueiredo, P.M., Malservisi, R., Dixon, T.H., 2018. A new geological slip rate estimate for the Calico Fault, eastern California: implications for geodetic versus geologic rate estimates in the Eastern California Shear Zone. Int. Geol. Rev. TIGR-2018-0129 (in review).

Ye, J., Liu, M., 2017. How fault evolution changes strain partitioning and fault slip rates in southern California: results from geodynamic modeling. J. Geophys. Res., Solid Earth 122 (8), 6893–6909. https://doi.org/10.1002/2017JB014325.